

# The seed energy fluctuation of hard X-ray self-seeding Free Electron Laser

C. Yang,<sup>1,2</sup> X. Wang,<sup>2,3</sup> C.-Y. Tsai,<sup>2,4</sup> G. Zhou,<sup>2,5</sup> Z. Zhang,<sup>2</sup> E. D. Krug,<sup>6</sup> A. Li,<sup>7</sup> H. Deng,<sup>3,8</sup> D. He,<sup>1</sup> and J. Wu<sup>2, a)</sup>

<sup>1)</sup>*National Synchrotron Radiation Laboratory, University of Science and Technology of China, Hefei 230029, China*

<sup>2)</sup>*SLAC National Accelerator Laboratory, Menlo Park, CA 94309, USA*

<sup>3)</sup>*Shanghai Institute of Applied Physics, CAS, Shanghai 201800, China*

<sup>4)</sup>*School of Electrical and Electronic Engineering, Huazhong University of Science and Technology, Wuhan, Hubei 430074, China*

<sup>5)</sup>*Institute of High Energy Physics, and UCAS, CAS, Beijing 100049, China*

<sup>6)</sup>*Seabreeze High School, 2700 N Oleander Ave, Daytona Beach, FL 32118, USA*

<sup>7)</sup>*Saratoga High School, 20300 Herriman Ave, Saratoga, CA 95070, USA*

<sup>8)</sup>*Shanghai Advanced Research Institute, CAS, Shanghai 201210, China*

(Dated: 15 March 2019)

Self-seeding free electron lasers (FELs) are capable of generating fully coherent X-ray pulses. However, the stability of output pulse energy of hard X-ray self-seeding (HXRSS) FEL is poor. This letter reports the seed energy stability investigation of HXRSS FEL. For the purpose of a more stable HXRSS FEL, this work suggests a relatively broad bandwidth  $\rho_t$  of crystal monochromator, a relatively long electron bunch with energy jitter(r.m.s.) down to a quarter of FEL Pierce parameter  $\rho$ , and a larger Bragg angle  $\theta_B$  to improve the seed energy stability. Moreover, the angle jitter (r.m.s.) between the SASE pulse incident direction and the crystal surface should be less than  $(\rho \tan \theta_B)/2$ , and the relative time jitter (r.m.s.) between the electron bunch and the seed should be less than half of the seed bump duration  $\mathcal{T}_t$ .

## I. INTRODUCTION

The successful operation of X-ray free electron lasers (FELs)<sup>1-3</sup> have offered unparalleled approaches for scientific study in many areas such as chemistry, biology, material science, atomic and molecular physics. As compared to the traditional third-generation synchrotron radiation light sources, FELs are characterized by ultra-short pulse length, high power output, and outstanding transverse coherence, tunable wavelength. To date, most of the existing short-wavelength FEL facilities, such as the Free-Electron LASer in Hamburg (FLASH)<sup>4</sup>, the Linac Coherent Light Source (LCLS)<sup>2</sup> and SPring-8 Angstrom Compact Free Electron Laser (SACLA)<sup>3</sup>, operate in the self-amplified spontaneous emission (SASE)<sup>5,6</sup> mode, which can generate stable output power ( $\sim 5\%$  r.m.s. fluctuations). For SASE FEL, the transverse coherence is excellent, but the temporal coherence is poor because of starting from shot noise.

In order to realize fully coherent FEL<sup>7</sup>, the external laser-seed FEL is proposed<sup>8</sup>. However, it is difficult to carry out external laser seeding in the X-ray regime. Therefore, self-seeding scheme was proposed in soft X-ray regime by employing a grating monochromator<sup>9</sup>, and later a self-seeding scheme with four-crystal monochromator was proposed in hard X-ray regime<sup>10</sup>. Afterwards, a more compact single crystal monochromator self-seeding scheme was proposed<sup>11</sup>, and has been successfully demonstrated at LCLS in 2012<sup>12</sup>. Although self-seeding scheme can generate fully coherent X-ray pulse, the stability of the output pulse energy is poor ( $\sim 50\%$

r.m.s. fluctuations)<sup>12</sup>. Such a large fluctuation still limit the application of HXRSS FEL.

In this work, we focus on the seed energy fluctuation investigation for a more stable single-crystal HXRSS FEL by numerical simulation. The pulse energy measured in experiment is after the saturation where includes the non-linear effect and the SASE contrast. That means it is difficult to find the reasons leading to the fluctuation of HXRSS FEL based on the measurement data. Therefore, we trace back to the monochromatic seed at the entrance of the FEL amplifier. The seed energy fluctuation can be caused by the intrinsic fluctuations of SASE, the bandwidth of the crystal monochromator, the electron bunch length, the electron bunch energy jitter, the jitter of the SASE incident angle on the crystal surface attributing to the crystal vibrations and SASE propagation direction jitter, the transverse and longitudinal overlap between the electron beam and seed.

TABLE I. Parameters of electron bunch and undulator.

Parameter	Value	Unit
Electron beam energy	9.5064	GeV
Energy spread	1.5	MeV
Peak current	3000	A
Normalized emittance	0.4	mm-mrad
Average beta function	15	m
Pierce parameter $\rho$	$6.91 \times 10^{-4}$	-
Undulator parameter $K$	2.4385	-
Undulator period	2.6	cm

<sup>a)</sup>Electronic mail: jhwu@slac.stanford.edu

## II. THEORETICAL AND NUMERICAL ANALYSES

The simulation parameters are based on the LCLS-II Cu-Linac electron beam with an ideal Gaussian distribution. We obtain the FEL pulses with the help of FEL simulation code GENESIS<sup>13</sup>. The seed is produced by the approach proposed by Geloni *et al*<sup>11</sup>. The SASE part consists of 10 undulator cells. The thickness of diamond monochromator is 110  $\mu\text{m}$ . The relevant simulation parameters are summarized in Table 1.

There are some numerical analyses showing the SASE pulse energy fluctuation decreases as a function of the ratio of the pulse length  $l$  over the coherence length  $l_c$ <sup>14</sup>. Yu *et al.* develop a theory of the SASE fluctuation<sup>15</sup>, and the fluctuation is theoretically given by

$$\frac{\sigma_E}{\bar{E}} = \frac{\sqrt{\frac{1}{N} \sum_{i=1}^N (E_i - \bar{E})^2}}{\bar{E}} \sim \frac{1}{\sqrt{l/l_c}}, \quad (1)$$

where  $N$ ,  $\sigma_E$ ,  $\bar{E}$ ,  $l$ , and  $l_c$  are the number of FEL pulses, the standard deviation of the pulse energy, the average pulse energy, the bunch length, the longitudinal coherence length of SASE pulse, respectively. For HXRSS FEL, the seed derives from the SASE pulse generated in the first undulator. Therefore, the seed has an intrinsic fluctuation inheriting from the SASE.

The seed energy fluctuation is firstly investigated as a function of the bandwidth of the crystal monochromator. Here,  $\rho_t$  and  $\rho_r$  are the normalized bandwidth (normalized by Bragg resonant photon energy) corresponding to the transmissive seed and the reflected seed<sup>16–18</sup>. The transmissive seed and the reflected seed are usually applied in HXRSS and X-ray FEL oscillator (XFELO)<sup>19–23</sup>, respectively.

$$\rho_r = \frac{P \sqrt{|b| \chi_h \chi_{\bar{h}}}}{\sin^2 \theta_B}, \quad \rho_t \simeq \frac{d}{2\pi \Lambda_0} \frac{P \sqrt{|b| \chi_h \chi_{\bar{h}}}}{\sin^2 \theta_B}, \quad (2)$$

where,  $\theta_B$ ,  $P$ ,  $b$ ,  $d$ ,  $\Lambda_0$  are the Bragg angle, the polarization factor, the asymmetry ratio of crystal, the crystal thickness, and the extinction length, respectively.  $\chi_h$  and  $\chi_{\bar{h}}$  are the Fourier coefficients of electric susceptibility. Figure 1 shows the seed energy fluctuation decreases as a function of the ratio of the crystal bandwidth  $\rho_t$  over the FEL Pierce parameter  $\rho$ .

The well-known FEL resonance condition is given by

$$\lambda_s = \lambda_u \frac{1 + K^2/2}{2\gamma_{er}^2}, \quad (3)$$

where  $\lambda_u$ ,  $\gamma_{er}$  are the undulator period and the resonant electron energy, respectively. The radiation frequency shift caused by electron energy jitter can be expressed as

$$\frac{\sigma_{\Delta\nu}}{\nu_s} = 2 \frac{\sigma_{\Delta\gamma_e}}{\gamma_{er}}, \quad (4)$$

where  $\nu_s$ ,  $\sigma_{\Delta\nu}$ ,  $\sigma_{\Delta\gamma_e}$  are the resonance frequency, the r.m.s. of central frequency jitter of SASE and the r.m.s. of electron energy jitter, respectively. If there is no electron energy jitter, the photons corresponding to central

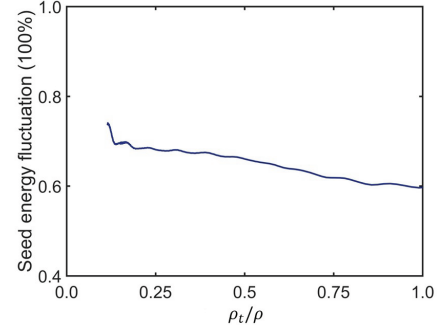


FIG. 1. Seed energy fluctuation decrease as the function of the ratio of  $\rho_t/\rho$ . Here, the crystal bandwidth  $\rho_t$  varies with the asymmetry ratio  $\gamma$  for the (111) reflecting atomic planes. We neglect other factors leading to the seed fluctuation.

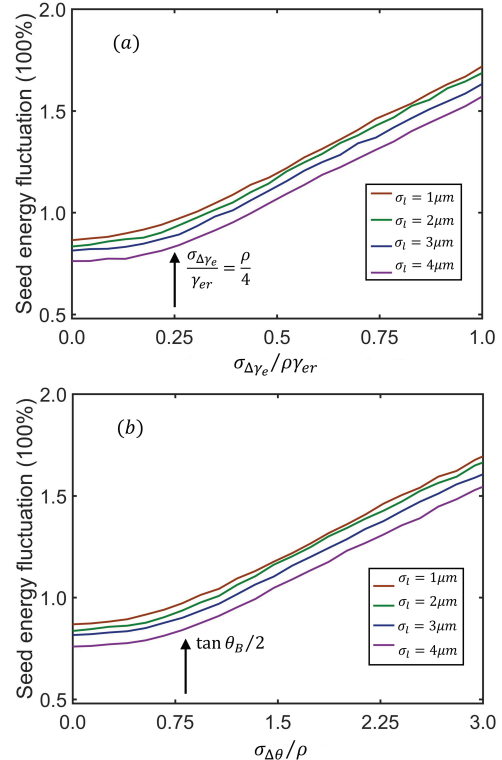


FIG. 2. (a) The seed energy fluctuation is induced by the electron beam energy jitter  $\sigma_{\Delta\gamma_e}$  (r.m.s.). (b) The seed energy fluctuation is caused by the angle jitter  $\sigma_{\Delta\theta}$  (r.m.s.). Here,  $\sigma_l$  is the standard deviation of electron bunch length. We use symmetry ( $\gamma = -1$ ) diamond (004) reflecting atomic planes, and the seed fluctuation caused by other factors are neglected.

photon energy of the radiation spectrum will contribute to the monochromatic seed. However, once the electron beam energy jitter is considered, the FEL spectrum would have a jitter. For this case, the photons contributing to the seed are not always the photons corresponding to the central photons.

Figure 2 (a) shows the seed energy fluctuation changes as a function of electron beam energy jitter for different bunch lengths. In order to reduce the seed energy fluctuation, the central frequency jitter should be within

the FEL bandwidth. In other words, the electron energy jitter(r.m.s.) should be less than  $\rho/4$ . Figure 2 also indicates that the seed energy fluctuation of long bunch is smaller than that of the short bunch.

For the investigation of seed energy fluctuation caused by angular jitter, we start from Bragg condition.

$$2d \sin \theta_B = \lambda_B, \quad (5)$$

where  $d$ ,  $\theta_B$ ,  $\lambda_B$  are the lattice constant, the Bragg angle and the Bragg resonant wavelength, respectively. The Bragg resonant frequency shift caused by the incident angle deviation can be expressed as

$$\frac{\sigma_{\Delta\nu}}{\nu_B} = -\cot \theta_B \sigma_{\Delta\theta}, \quad (6)$$

where  $\nu_B$ ,  $\sigma_{\Delta\nu}$ ,  $\sigma_{\Delta\theta}$  are the Bragg resonant frequency, the r.m.s of Bragg resonant frequency jitter, and the r.m.s of the angle jitter between the SASE incident direction and the crystal surface (angle jitter).

Figure. 2 (b) shows the seed energy fluctuation variations as a function of the angle jitter. For the purpose of more stable HXRSS FEL, the angle jitter  $\sigma_{\Delta\theta}$  is less than  $(\rho \tan \theta_B)/2$ . Moreover, we find that the average bandwidth of the seed is broadened because of the angle

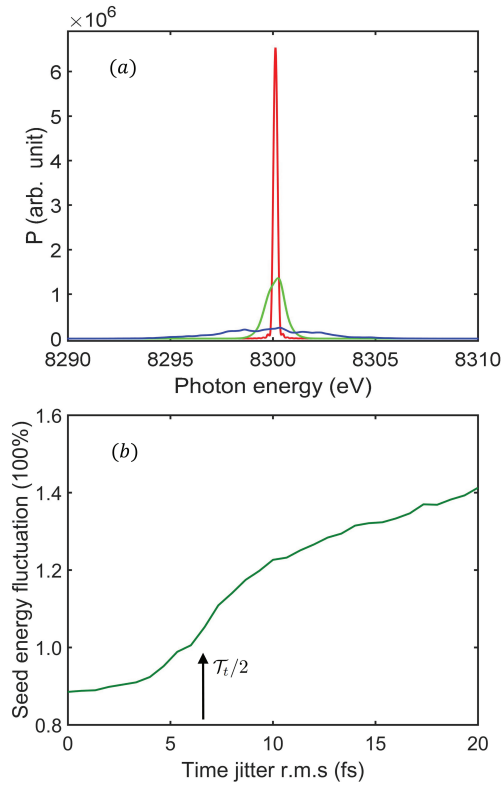


FIG. 3. (a) The average bandwidth of seed is broadened because of the angle jitter between the SASE propagation direction and the crystal surface. The red curve is the single shot. The green and blue curves refer to  $\sigma_{\Delta\theta} \approx 92\mu\text{rad}$  and  $\sigma_{\Delta\theta} \approx 554\mu\text{rad}$ . (b) The seed fluctuation resulting from the relative time jitter  $\sigma_t$  (r.m.s.). Here, we used symmetry ( $\gamma = -1$ ) diamond (004) reflecting atomic planes, and the seed fluctuations induced by other processes are ignored.

jitter shown in Fig. 3 (a). Of particular concern, the angle jitter(r.m.s.) should be smaller than half of the Darwin width for XFEL and cascade HXRSS FEL<sup>24</sup>. In addition, a larger Bragg angle  $\theta_B$  can help to improve the tolerance of the angle jitter of the machine.

The longitudinal and transver overlap between the seed and electron beam can also contribute to the seed energy fluctuation. It should be noted that the seed has a spatiotemporal coupling<sup>17,18</sup>, which is described by

$$\Delta x = c \Delta t \cot \theta_B, \quad (7)$$

where  $\Delta x$ ,  $c$ ,  $\Delta t$  are the transverse shift of seed, the speed of light, and the time delay, respectively. A larger Bragg angle  $\theta_B$  benefits the transverse overlap between the seed and electron beam.

As for the longitudinal overlap between the electron beam and seed, we assume the relative time jitter obeys normal distribution. Figure 3 (b) shows the simulation result. To improve the stability of HXRSS, the time jitter(r.m.s) should be less than half of the seed bump duration  $\mathcal{T}_t/2$  ( $\mathcal{T}_t = 1/(\rho_t \nu_B)$ ). For XFEL, the time jitter(r.m.s) should be less than  $\mathcal{T}_r/2$  ( $\mathcal{T}_r = 1/(\rho_r \nu_B)$ ).

### III. SUMMARY AND DISCUSSION

In conclusion, we have reported the factors that affect the seed energy stability in HXRSS FEL. The numerical analyses show that a crystal monochromator with relatively broad bandwidth  $\rho_t(\rho_r)$  can reduce the fluctuation of seed energy. Furthermore, a relatively longer electron bunch length  $l$  can also benefit to improve the stability of seed energy. Moreover, a larger Bragg angle  $\theta_B$  not only improves the tolerance of the angle jitter, but also elevates the transverse overlap between the electron bunch and seed. In addition, in order to further improve the stability of seed energy, the electron beam energy jitter(r.m.s.) should be less than  $\rho/4$ , and the angle jitter should be less than  $(\rho \tan \theta_B)/2$ , and the relative time jitter between the electron beam and seed should be less than  $\mathcal{T}_t/2$ . We also found that the angle jitter broaden the average bandwidth of the seed. In our simulation case, the Bragg resonance photon energy is 8300 eV, and diamond (004) is chosen. The Pierce parameter  $\rho \approx 6.91 \times 10^{-4}$ . Hence, the electron energy jitter (r.m.s.) should be less than  $\rho/4 \approx 0.017\%$ . The Bragg angle  $\theta_B \approx 21.27^\circ$ , and the angle jitter (r.m.s) should be less than  $(\rho \tan \theta_B)/2 \approx 130\mu\text{rad}$ . The seed bump duration  $\mathcal{T}_t \approx 14\text{fs}$ , and the time jitter (r.m.s.) should be less than  $\mathcal{T}_t/2 \approx 7\text{fs}$ . However, for LCLS machine, the electron energy jitter is 0.04%, and the time jitter is 50 fs. The two parameters are larger than the limits given in this paper, which results in the large fluctuation of HXRSS FEL. Therefore, a more stable HXRSS FEL calls on a more stable accelerator system with smaller electron energy jitter, time jitter, and angular jitter.

## ACKNOWLEDGEMENTS

The work was supported by the US Department of Energy (DOE) under contract DE-AC02-76SF00515 and the US DOE Office of Science Early Career Research Program grant FWP-2013-SLAC-100164.

## REFERENCES

- <sup>1</sup>V. Ayvazyan, N. Baboi, *et al.*, The European Physical Journal D - Atomic, Molecular, Optical and Plasma Physics **37**, 297 (2006).
- <sup>2</sup>P. Emma, R. Akre, *et al.*, Nature Photonics **4**, 641–647 (2010).
- <sup>3</sup>T. Ishikawa, H. Aoyagi, *et al.*, Nature Photonics **6**, 540 (2012).
- <sup>4</sup>W. Ackermann, G. Asova, *et al.*, Nature Photonics **1**, 336 (2007).
- <sup>5</sup>A. M. Kondratenko and E. L. Saldin, Part. Accel. **10**, 207 (1980).
- <sup>6</sup>R. Bonifacio, C. Pellegrini, and L. Narducci, Optics Communications **50**, 373 (1984).
- <sup>7</sup>C. Feng and H. Deng, Nuclear Science and Techniques **29**, 2916001 (2018).
- <sup>8</sup>L. H. Yu, Phys. Rev. A **44**, 5178 (1991).
- <sup>9</sup>J. Feldhaus, E. Saldin, J. Schneider, E. Schneidmiller, and M. Yurkov, Optics Communications **140**, 341 (1997).
- <sup>10</sup>E. L. Saldin, E. A. Schneidmiller, Y. V. Shvydko, and M. V. Yurkov, AIP Conference Proceedings **581**, 153 (2001).
- <sup>11</sup>G. Geloni, V. Kocharyan, and E. Saldin, Journal of Modern Optics **58**, 1391 (2011).
- <sup>12</sup>J. Amann, W. Berg, *et al.*, Nature Photonics **6**, 693 (2012).
- <sup>13</sup>S. Reiche, Nuclear Instruments and Methods in Physics Research Section A: Accelerators, Spectrometers, Detectors and Associated Equipment **429**, 243 (1999).
- <sup>14</sup>R. Bonifacio, L. De Salvo, P. Pierini, N. Piovella, and C. Pellegrini, Phys. Rev. Lett. **73**, 70 (1994).
- <sup>15</sup>L. H. Yu and S. Krinsky, Nuclear Instruments and Methods in Physics Research Section A: Accelerators, Spectrometers, Detectors and Associated Equipment **407**, 261 (1998).
- <sup>16</sup>A. Authier, *Dynamical theory of X-ray diffraction* (Oxford University Press, 2001).
- <sup>17</sup>R. Lindberg and Y. V. Shvyd'ko, Phys. Rev. ST Accel. Beams **15**, 050706 (2012).
- <sup>18</sup>Y. Shvyd'ko and R. Lindberg, Phys. Rev. ST Accel. Beams **15**, 100702 (2012).
- <sup>19</sup>R. R. Lindberg, K.-J. Kim, Y. Shvyd'ko, and W. M. Fawley, Phys. Rev. ST Accel. Beams **14**, 010701 (2011).
- <sup>20</sup>K.-J. Kim, Y. V. Shvydko, and R. Lindberg, Synchrotron Radiation News **25**, 25 (2012).
- <sup>21</sup>K. Li and H. Deng, Phys. Rev. Accel. Beams **20**, 110703 (2017).
- <sup>22</sup>K. Li, J. Yan, C. Feng, M. Zhang, and H. Deng, Phys. Rev. Accel. Beams **21**, 040702 (2018).
- <sup>23</sup>K. Li and H. Deng, Appl. Phys. Lett. **113**, 061106 (2018).
- <sup>24</sup>G. Geloni, V. Kocharyan, and E. Saldin, (2011), arXiv:1109.5112 [physics.acc-ph].

